Electronic Supplementary Material (ESI) for ChemComm.

Supporting Information

A Bioinspired Oxoiron(IV) Motif Supported on a N_2S_2 Macrocyclic Ligand

Jennifer Deutscher,[a] Philipp Gerschel,[b] Katrin Warm,[a] Uwe Kuhlmann,[c] Stefan Mebs,[d] Michael Haumann,[d] Holger Dau,[d] Peter Hildebrandt,[c] Ulf-Peter Apfel*[b] and Kallol Ray*[a]

Experimental Procedures

Chemicals, materials and instrumentation

Chemicals and handling. The chemicals employed were purchased from the companies ABCR, ACROS, Sigma-Aldrich and TCI, and used without further purification. Anhydrous solvents (acetonitrile, diethylether, dichloromethane and acetone) were purchased from CARL-Roth GmbH under the tradename ROTIDRY (>99.5%, <50% ppm H_2O), degassed by freeze-pump-thaw-methods prior to use and stored over activated molecular sieves. Deuterated solvents were purchased from EURISO-TOP.

Preparation and handling of air or water sensitive compounds were performed under an inert atmosphere using either Schlenk techniques or a GS MEGA E-Line glovebox from GS Glovebox Systemtechnik filled with N_2. Nitrogen and Argon of quality 5.0 were used for this purpose and were purchased from AIR LIQUIDE.

Elemental analysis. All elemental analyses were performed by the analytical service of the Institut für Chemie of the Humboldt-Universität zu Berlin. The percentages of Carbon, Hydrogen, Nitrogen and Sulphur were determined using an HEKAtech EURO EA 3000 analyzer. The reported values are the result of an average of two independent measurements except for Fluorine analysis, where only one measurement was performed

Nuclear magnetic resonance spectroscopy. All NMR spectra were recorded using a BRUKER 300 DPX spectrometer equipped with a cryostat. Those of ^{1}H and ^{19}F nuclei were recorded in deuterated solvents, and chemical shifts (ppm) referenced against residual protic solvent peaks. For low temperature measurements a freshly melted solution of **1-*trans*** was inserted into the precooled spectrometer and measured at -85 °C with a spectrometer radiofrequency F of 300 MHz.

Electrospray ionization mass spectrometry. ESI-MS spectra of organic molecules and inorganic complexes in solution were recorded by using an ADVION EXPRESSION CMS spectrometer (under "typical" ionization conditions) and spectra in positive and negative modes were collected in parallel; acetonitrile was used as an eluent. The analysis of the data was carried out with the ADVION DATA EXPRESS Version 6.0.11.3. For thermally unstable complexes, ESI-MS spectra were recorded by using an AGILENT TECHNOLOGIES 1200 MASS spectrometer. Freshly thawed solutions were directly injected into the instrument while the ionization source temperature was decreased to 40°C. The analysis of the data was carried out with the AGILENT MASSHUNTER QUALITATIVE ANALYSIS software version B.02.00.

Gaschromatography. GC analysis was carried out by using an AGILENT 7890B gas chromatograph (HP5 25 column, 30 m) with a flame-ionization detector. GC-MS was performed on an AGILENT 5977B spectrometer with a triple-axis detector.

Single crystal X-ray structure determinations. For the determination of the X-ray crystal structures of the complexes data collection was performed at 100 K on a BRUKER D8 VENTURE diffractometer by using Mo K_α radiation (λ = 0.71073 Å). Multi-scan absorption corrections implemented in SADABS[1] were applied to the data. The structure was solved by intrinsic phasing method (SHELXT 2014/5)[2] and refined by full matrix least square procedures based on F_2 with all measured reflections (SHELXL-2018/3)[3] in the graphical user interface SHELXle[4]) with anisotropic temperature factors for all non-hydrogen atoms. All hydrogen atoms were added geometrically and refined using a riding model. **1a-*cis*** was refined as an inversion twin using the PLATON software.[5]

CCDC 2054129 (**1a-*cis***) and **CCDC 2054130** (**1a-*trans***) contain the supplementary crystallographic data for this paper. These data can be obtained free of charge from the Cambridge Crystallographic Data Centre via www.ccdc.cam.ac.uk/data_request/cif.

Mößbauer spectroscopy. Mößsbauer spectra in the absence of magnetic field were recorded on a SEECO MS6 spectrometer that comprises the following instruments: a JANIS CCS-850 cryostat, including a CTI-CRYOGENICS closed cycle 10K refrigerator, and a CTI-CRYOGENICS 8200 helium compressor. The cold head and sample mount are equipped with calibrated DT-670-Cu-1.4L silicon diode temperature probes and heaters. Temperature is controlled by a LAKESHORE 335 temperature controller. Spectra are recorded using a LND-45431 Kr gas proportional counter with beryllium window connected to the SEECO W204 γ-ray spectrometer that includes a high voltage supply, a 10 bit and 5 µs ADC and two single channel analyzers. Motor control and recording of spectraare taken care of by the W304 resonant γ-ray spectrometer. For the reported spectra a RIVERTEC MCO7.114 source (^{57}Co in Rh matrix) with an activity of about 1 GBq was used. All spectra were recorded in a plastic sample holder with a frozen solution sample at 15 K and data were accumulated for about 12 to 24 hours.

X-ray absorption spectroscopy. XAS at the Fe K-edge was performed at beamline KMC-3 at the BESSY-II synchrotron (Helmholtz Center Berlin, Germany) as described earlier[6] using a set-up including a Si[111] double-crystal monochromator, a 13-element energy-resolving Si-drift detector (RaySpec) for X-ray fluorescence monitoring, and DXP-XMAP pulse-processing electronics (XIA). Samples were held at 20 K in a liquid-helium cryostat (Oxford). The energy axis of the monochromator was calibrated (accuracy ±0.1 eV) using the K-edge spectrum of an iron metal foil (fitted reference energy of 7112 eV in the first derivative spectrum). The spot size on the samples was ca. 1.5 x 5.0 mm (vertical x horizontal) as set by a focusing mirror and slits. X-ray fluorescence spectra were collected using a continuous scan mode of the monochromator (scan duration ~10 min). Up to 6 scans were averaged (1-2 scans per sample spot) for signal-to-noise ratio improvement. XAS data were processed (dead-time correction, background subtraction, normalization) to yield XANES and EXAFS spectra using our earlier described procedures and in-house software.[7] k^3-weighted EXAFS spectra were simulated with in-house software and phase functions from FEFF9 ($S_0^2 = 0.8$).[8] EXAFS simulation results are tabulated in Table S4.

Resonance Raman (rRaman). Resonance Raman spectra were measured from a 95:5 mixture of CD_2Cl_2 and CD_3CN at –90 °C (Linkam cryostat) using 413 nm excitation from a Kr^+-laser (5 mW) with a Horiba Jobin-Yvon LabRAM HR800 confocal Raman spectrometer. The sample concentrations employed were 4 mM.

Cyclovoltammetry. Cyclovoltammetry was performed in a TSC 1600 CLOSED cell setup from RHD INSTRUMENTS connected with an AUTOLAB PGSTAT204 potentiostat from METROHM. The cell was equipped with a Pt-working electrode (0.25 mm diameter) and a Pt counter electrode. Another Pt electrode was used as reference. Best results were received using a scan-rate of 0.5 V/s and a step size of 0.015 V. All voltammetries have been carried out with $n\mathrm{Bu}_4\mathrm{NPF}_6$ (TBAP) as supporting electrolyte (0.1 M ionic strength) in CH_3CN under inert conditions and referenced by the ferrocenium/ferrocene redox couple.

Syntheses

1,8-dithia-4,11-diazacyclotetradecane (Dithiacyclam). Dithiacyclam was prepared as described in the literature.[9]

[(dithiacyclam)Fe(OTf)$_2$] (1a-*cis*) and [(dithiacyclam)Fe(MeCN)$_2$][(OTf)$_2$] (1a-*trans*). Dithiacyclam (25 mg, 0.107 mmol) was added to a solution of $Fe(MeCN)_2(OTf)_2$ (44 mg, 0.1 mmol) in 1 mL MeCN under an inert atmosphere at 20 °C and stirred for 2h. The blue solution was filtered and precipitated by the addition of Et_2O. The light beige solid formed was isolated and dried under vacuum overnight (42 mg, 0.07 mmol, 72%). Crystals suitable for X-ray diffraction analysis were grown by vapour diffusion of Et_2O into a solution of the complex in MeCN at -15 °C (**1a-*cis***) and -40 °C (**1a-*trans***). CHNS analysis (**1a-*cis***): exp.: C: 24.43, H: 3.69, N: 4.7, S: 22.19, calc.: C: 24.49, H: 3.77, N: 4.76, S: 21.8. ESI-MS (MeCN, pos. mode): $[Fe(dithiacyclam)OTf]^+$ *m/z* calc. 439.0; found 439.0.

Syntheses of ^{57}Fe-enriched 1a-*cis* and 1a-*trans*. ^{57}Fe-enriched **1a-*cis*** and **1a-*trans*** were necessary for performing Mößbauer studies in solution. In order to synthesize the ^{57}Fe-enriched **1a-*cis*** and **1a-*trans***, $^{57}Fe(MeCN)_2(OTf)_2$ was generated first. In an inert atmosphere, metallic ^{57}Fe (42 mg, 0.74 mmol) and a degassed concentrated HCl solution (4 mL) were stirred at 65 °C overnight until all the iron was dissolved. The solvent was then removed by vacuum and the resultant white residue was suspended in dry CH_3CN (4 mL). $(CH_3)_3Si(OTf)$ (820 mg, 3.69 mmol) in dry CH_3CN (2 mL) was added dropwise over a period of 2 minutes. The resultant solution was stirred overnight and the solvent was removed by vacuum. The remaining solid was redissolved in a minimum amount of dry CH_3CN and an excess of dry Et_2O was added. The mixture was left overnight at -20 °C during which time white crystals were formed. The crystals were filtered, washed with dry Et_2O and dried. $^{57}Fe(MeCN)_2(OTf)_2$ was obtained as a white solid. Yield: 175mg (0.4 mmol, 55%). This product was directly employed in the syntheses of ^{57}Fe-enriched **1a-*cis*** and **1a-*trans***; the procedure described for the synthesis of **1a-*cis*** and **1a-*trans*** was followed, using $^{57}Fe(MeCN)_2(OTf)_2$ instead of $Fe(MeCN)_2(OTf)_2$.

2-(tert-butylsulfonyl)-iodosylbenzene (^{s}PhIO). ^{s}PhIO was synthesized according to previously reported procedures.[10] The ^{18}O-labelled ^{s}PhI^{18}O was synthesized as follows: A 1 M solution of $Na^{18}OH$ was prepared by the addition of NaH (40 mg, 1 mmol) to $H_2{}^{18}O$ under an inert atmosphere. 2-(tert-butylsulfonyl)(diacetoxyiodo)benzene (300 mg, 0.7 mmol) was added in small portions and the mixture was stirred for 30 min at 20 °C. The aqueous phase was removed by filtration through Teflon-tubes and washed with 0.5 mL portions of $H_2{}^{18}O$ until the pH was neutral. The pale-yellow solid was then washed twice with anhydrous Et_2O and dried under vacuum (186 mg, 0.56 mmol, 80%). ^{1}H-NMR (300 MHz, $CDCl_3$): δ = 8.11 (d, J = 7.8 Hz, 1H), 7.90 – 7.80 (m, 2H), 7.66 – 7.58 (m, 1H), 1.41 (s, 9H) ppm.

Sample preparations

In a typical experiment, 2 mL of a solution of the Fe^{II} complex **1a-*trans*** in a 95:5 mixture of DCM and MeCN was cooled to -90 °C in a UV-Vis quartz cuvette (10 mm pathlength) and a solution of 4 eq ^{s}PhIO, dissolved in 0.1 mL DCM, was injected into the solution. The formation of the intermediate **1-*trans*** was monitored by UV-Vis following the bands at 596 nm and 815 nm. The samples were transferred into precooled sample holders as soon as the formation was complete. λ_{max} (ε_{max}): 596 nm (226 $M^{-1}cm^{-1}$), 815 nm (549 $M^{-1}cm^{-1}$), ESI-MS (pos. mode): m/z $[(dithiacyclam)Fe(O)(OTf)]^+$ exp. 455.0; calc. 455.0.

Samples for XAS (4mM) and Mößbauer spectroscopy (2 mM) were prepared from a Fe^{II} solution in a 95:5 mixture of DCM and MeCN and were diluted with acetone to decrease the amount of DCM. Samples for rRaman (4 mM) and ESI-MS (1 mM) were prepared in an undiluted 95:5 mixture of DCM and MeCN. Samples for NMR (4 mM) were prepared either in d_6-Acetone (**1a-*cis***) or in a 95:5 mixture of d_2-DCM and d_3-MeCN (**1a-*trans*** and **1-*trans***).

GC-MS samples for analysis of the organic products were prepared by addition of substrate (5 eq for xanthene, DHA and triphenylphosphine) in 0.1 mL solvent to a 0.5 mM solution of **1-*trans*** at -80 °C and -65 °C (for fluorene and indene). After the decay of the 815 nm band was confirmed by UV-Vis spectroscopy, the solutions were warmed to room temperature, quenched by the addition of Na_2SO_3, a known amount of biphenyl was added as an internal standard and the solutions were filtered through a short plug of silica and $MgSO_4$ to remove the metal complex and traces of water.

Reactivity studies were performed either at -80 °C or -65 °C with 1 mM concentration of **1-*trans***. After addition of the substrates (>20 eq) to a preformed solution of **1-*trans*** the decay of the 815 nm band was monitored over 250 s and fitted with pseudo-first order kinetics to obtain k_{obs} values. Plotting the k_{obs} values over several concentrations and employing a linear fit yielded k_2 values. The k_2 values were normalized by the number of equivalent H atoms (k_2') in order to correlate them to the bond dissociation energies (BDE) of the corresponding C-H bonds.

Hydrogen/Deuterium Kinetic isotope effects (KIEs) were determined as the ratio of the k_2 value measured for the substrate containing exclusively C-H bonds and the k_2 value obtained from the deuterated substrate.

Computational details:

Starting from the XRD-coordinates of compound **1a-*trans*** and the corresponding precursor of **2-*trans***, DFT calculations were conducted at the BP86/TZVP level of theory applying Gaussian16.[11] Dispersion was taken into account for by the empirical dispersion correction of Grimme.[12] The COSMO solvation model was used to mimic the acetonitrile solvent.

Results and Discussion

Spectroscopic studies

Table S1. Selected bond lengths and distances in **1a-*cis***.

Atoms	d [Å]	Atoms	Angles [°]
Fe1-O4	2.094(3)	O4-Fe1-O1	87.84(13)
Fe1-O4	2.192(3)	O4-Fe1-N2	178.81(15)
Fe1-N2	2.198(4)	O1-Fe1-N2	91.11(14)
Fe1-N1	2.219(4)	O4-Fe1-N1	85.24(14)
Fe1-S2	2.4652(13)	O1-Fe1-N1	172.97(13)
Fe1-S1	2.4662(15)	N2-Fe1-N1	95.80(14)
		O4-Fe1-S2	88.30(11)
		O1-Fe1-S2	96.37(9)
		N2-Fe1-S2	92.35(11)
		N1-Fe1-S2	84.67(11)
		O4-Fe1-S1	95.60(11)
		O1-Fe1-S1	86.23(9)
		N2-Fe1-S1	83.80(11)
		N1 Fe1 S1	93.21(11)
		S2 Fe1 S1	175.40(5)

Table S2. Selected bond lengths and distances in the asymmetric unit of **1a-*trans*** (atoms N1’, N2’ and S1’ are symmetry equivalent with atoms N1, N2 and S1 due to the symmetry elements within the space group).

Atoms	d [Å]	Atoms	Angles [°]
Fe1-N1 Fe1-N1’	1.9246(18)	N1-Fe1-N2	87.83(7)
Fe1-N2 Fe1-N2’	2.0457(18)	N1’-Fe1-N2	92.17(7)
Fe1-S1 Fe1-S1’	2.2522(6)	N1-Fe1-S1	88.73(5)
		N1’-Fe1-S1	91.27(5)
		N2-Fe1-S1	92.87(5)
		N2’-Fe1-S1	87.13(5)
		N1-Fe1-N1’ N2-Fe1-N2’ S1-Fe1-S1’	180.0

Table S3. Crystallographic Data for **1a-*cis*** and **1a-*trans***.

	1a-*cis*	**1a-*trans***
Space group	P n a 2_1	P -1
Unit cell parameters	a = 18.5420(9) Å b = 14.0911(7) Å c = 8.2672(4) Å α = 90° β = 90° γ = 90° V = 2160.03(18) Å³	a = 8.5286(7) Å b = 8.8855(7) Å c = 9.7499(8) Å α = 96.876(4)° β = 90.559(3)° γ = 113.841(3)° V = 669.57(10) Å³
Z	4	1
Sum formula	C12 H22 F6 Fe N2 O6 S4	C16 H28 F6 Fe N4 O6 S4
Temperature	100(2) K	100(2) K
Total number of reflections collected (reflections with $I > 2\sigma(I)$)	3991 (3389)	2388 (2158)
Number of parameters/restraints	281/1	170/0
ϑ_{min}, ϑ_{max}	2.86, 25.84°	2.53, 25.07°
F (0 0 0)	1200	344
Crystal dimensions [mm x mm x mm]	0.32 x 0.12 x 0.04	0.24 x 0.14 x 0.14
Absorption coefficient μ	1.169	0.956
h, *k*, *l* range	$-22 < h < 22$ $-17 < k < 13$ $-10 < l < 9$	$-10 < h < 10$ $-10 < k < 10$ $-11 < l < 11$
R factor	0.0341	0.0289
wR factor	0.0591	0.0615
Goodness of Fit (GooF)	1.047	1.083

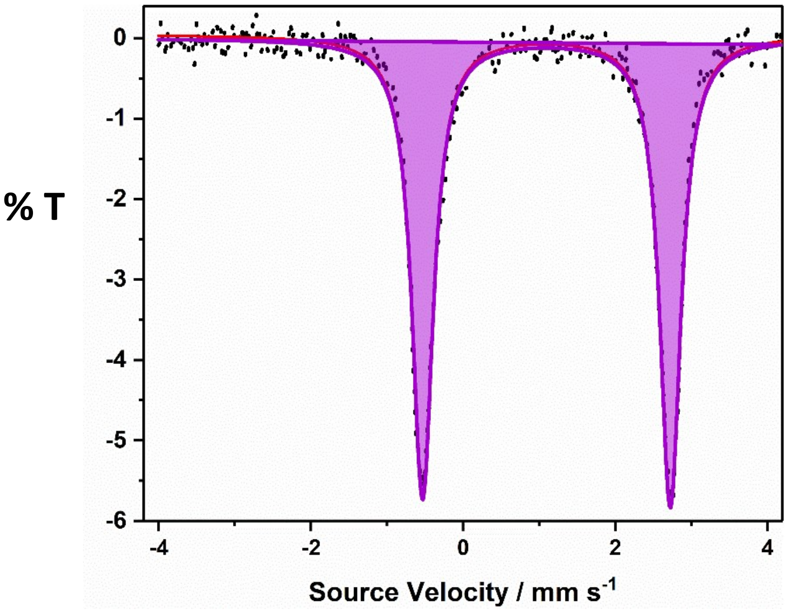

Figure S1. Zero-field Mössbauer spectrum of **1a-*cis*** in acetone at 15 K displaying an isomer shift of δ = 1.10 mm s^{-1} and quadrupole splitting of ΔE_Q = 3.26 mm s^{-1}.

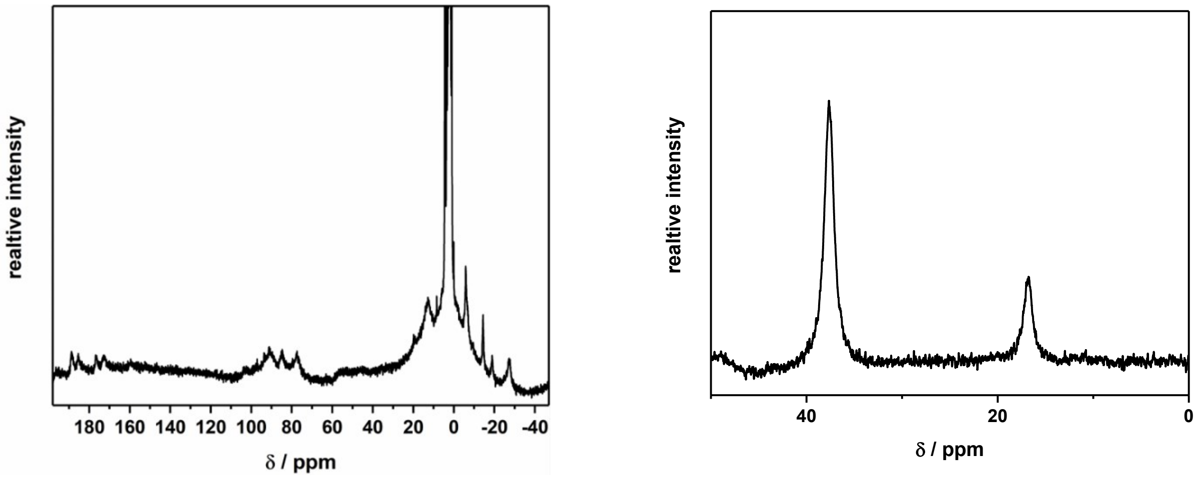

Figure S2. Left: ^{1}H-NMR spectrum of **1a-*cis*** in d_6-acetone at –85 °C displaying paramagnetically shifted peaks; right: ^{19}F-NMR spectrum of **1a-*cis*** in d_6-acetone at -85 °C displaying 2 signals corresponding to bound triflate anion(s).

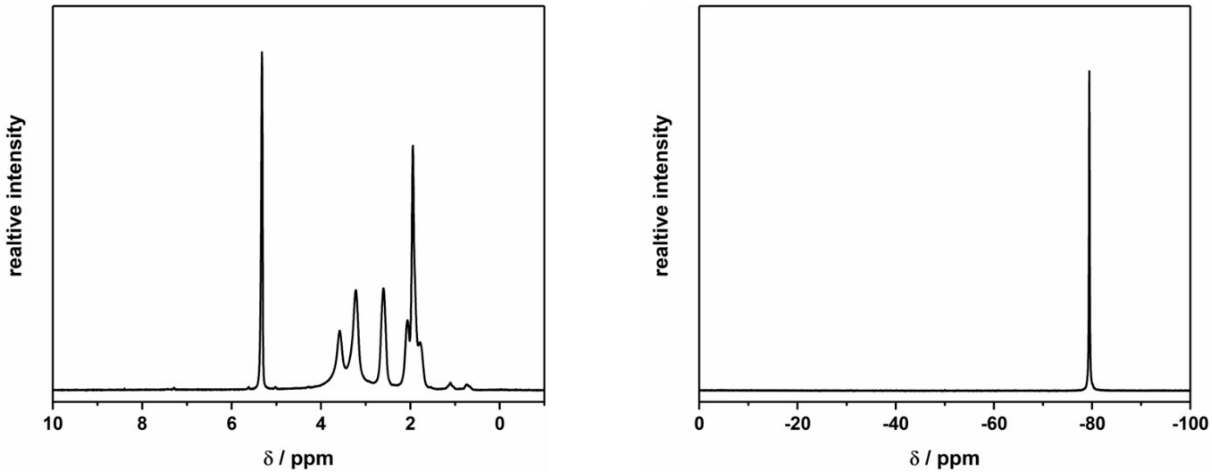

Figure S3. Left: ^{1}H-NMR spectrum of **1a-*trans*** in a 95:5 mixture of CD_2Cl_2 and CD_3CN at –85 °C displaying signals in the range of 0 to 4 ppm consistent with a S=0 ground state; right: ^{19}F-NMR spectrum of **1a-*trans*** in a 95:5 mixture of CD_2Cl_2 and CD_3CN at –85 °C displaying only 1 signal at –79 ppm corresponding to free triflate anion(s).

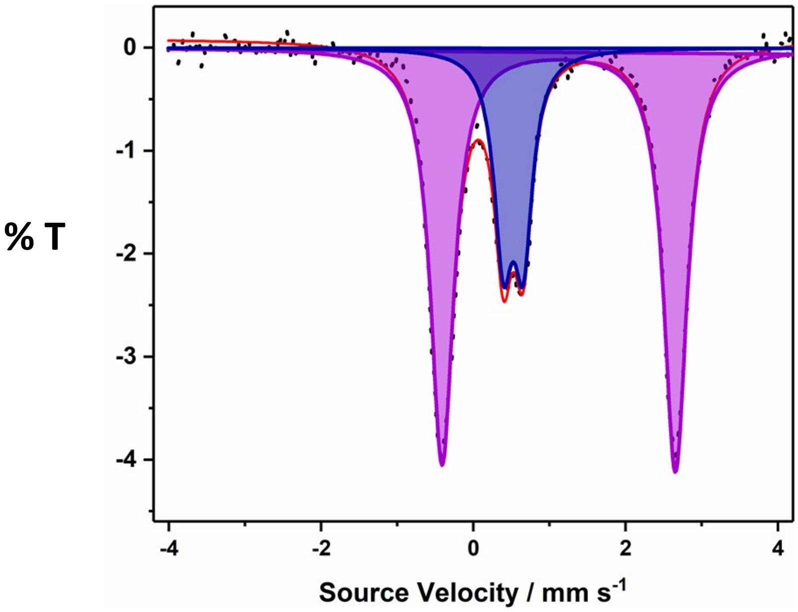

Figure S4. Zero-field Mößbauer spectrum of **1a-*trans*** in a mixture of acetone/DCM/MeCN (10:0.95:0.05) at 15 K displaying 2 species; purple: isomer shift of δ = 1.15 mm s^{-1} and quadrupole splitting of ΔE_{Q} = 2.31 mm s^{-1} and blue: isomer shift of δ = 0.52 mm s^{-1} and quadrupole splitting of ΔE_{Q} = 0.26 mm s^{-1}.

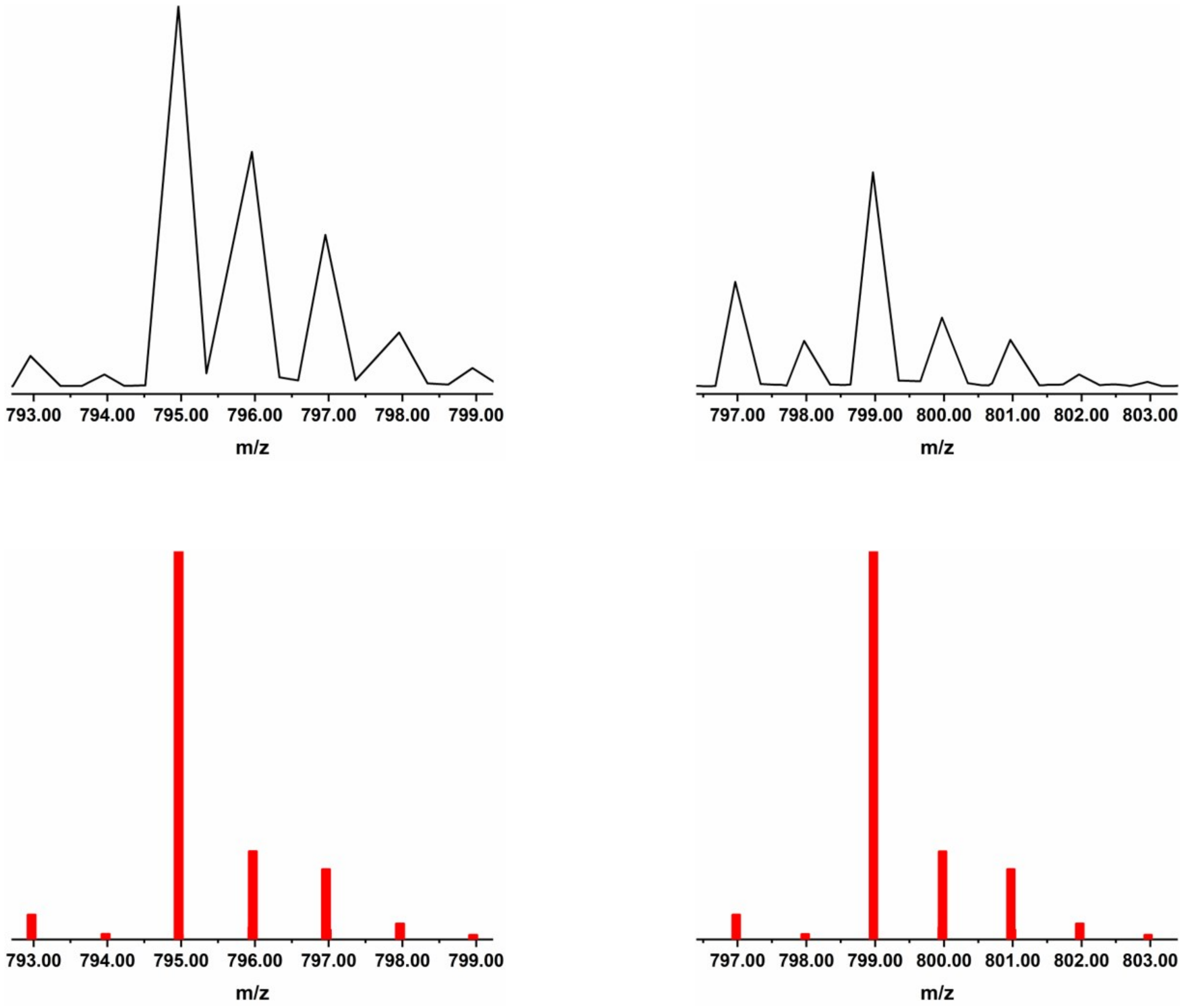

Figure S5. ESI-MS signals obtained for a freshly melted solution of **1-*trans*** and ^{18}O-enriched **1-*trans*** with decreased capillary temperature (+40 °C) (top: shows peak at *m/z* [(dithiacyclam)Fe^{IV}(O)(OTf)(^{s}PhIO)]$^{+}$ 794.96 (calc. 794.97) and at *m/z* [(dithiacyclam)Fe^{IV}(^{18}O)(OTf)(^{s}PhI^{18}O)]$^{+}$ 798.96 (calc. 798.98); bottom: calculated isotope pattern for the depicted species).

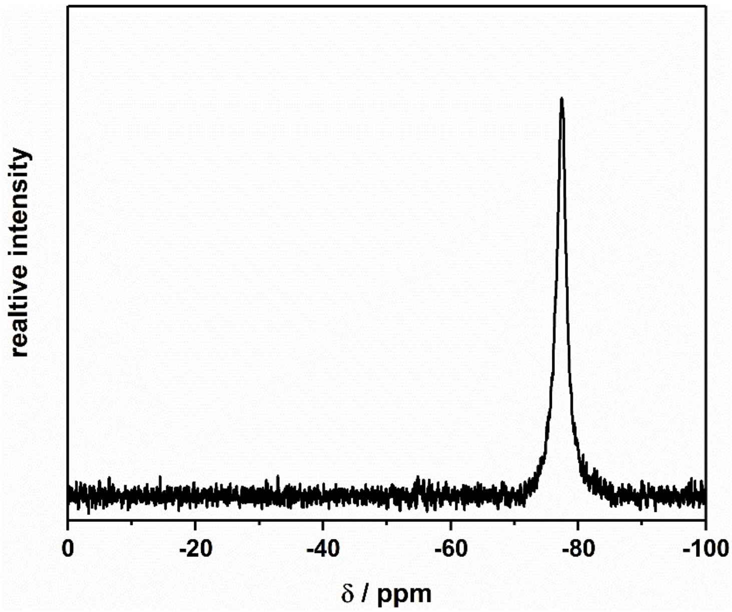

Figure S6. ^{19}F-NMR spectrum of **1-*trans*** at –85 °C displaying one signal at –77 ppm corresponding to free triflate anion(s).

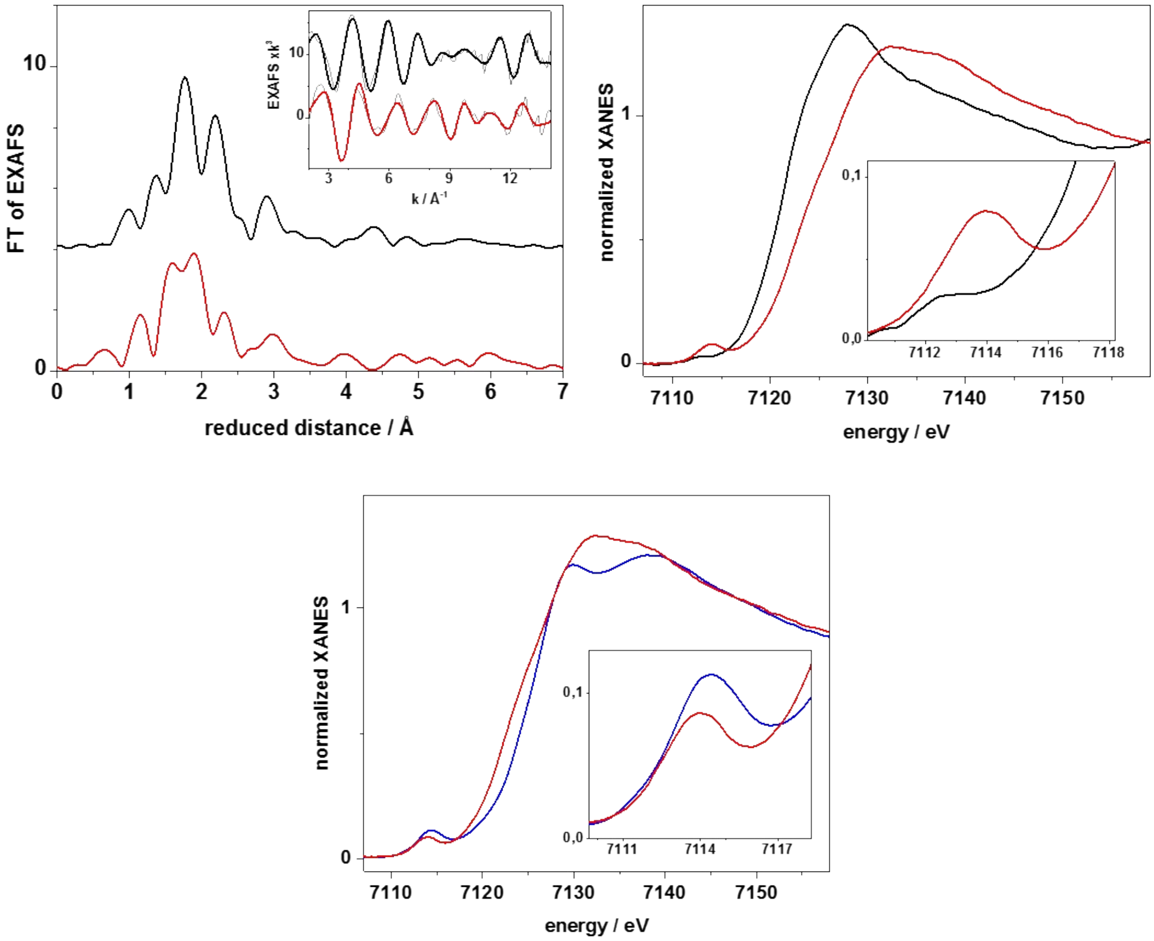

Figure S7. Top, left: Fourier-transforms (FT) of the experimental extended X-ray absorption fine structure (EXAFS) data of **1a-*trans*** (black) and **1-*trans*** (red); the inset shows the k^3-weighted EXAFS spectra on a wavevector (k) scale (grey lines, experimental data; black and red lines, simulations with parameters in Table S4). Top, right: Normalized X-ray absorption near edge structure (XANES) spectra of **1a-*trans*** (black) and **1-*trans*** (red) in an acetone/DCM/MeCN (10:0.95:0.05) solution featuring an edge energy (at 50 % level) of 7120.4 eV for **1a-*trans*** and 7122.7 eV for **1-*trans***, the inset shows the respective 1s→3d pre-edge features in the XANES. Bottom: comparison of XANES spectra of **1-*trans*** (red) and **2-*trans*** (blue) with an edge energy of 7123.9 eV.[6]

Table S4. EXAFS fit parameters. In parentheses are given the DFT calculated distances for **1-*trans*** in the S=1 state.

	shell	N [per Fe]	R [Å]	$2\sigma^2 \cdot 10^3$ [Å^2]	R_F (1-3 Å) [%]
1a-*trans*	Fe-N	2*	1.95	9[§]	14.3
	Fe-N	2.2[#]	2.12	2[&]	
	Fe-S	2*	2.37	9[§]	
	Fe-C	2.2[#]	2.71	2[&]	
	Fe-C	3*	3.17	3	
1-*trans*	Fe=O	0.7[#]	1.67 (1.66)	2*	15.3
	Fe-N	2*	1.88 (2.06)	9[§]	
	Fe-N	1.3[#]	2.01 (2.03)	2[§]	
	Fe-S	2*	2.25 (2.29)	9[§]	
	Fe-C	1.3[#]	2.77	2[§]	
	Fe-C	3*	3.46	7	

*Parameters that were fixed, [#]N-values that were coupled to a sum of 2 or to equal values, and [&]Debye-Waller factors that were coupled to equal values in the EXAFS fit procedure.

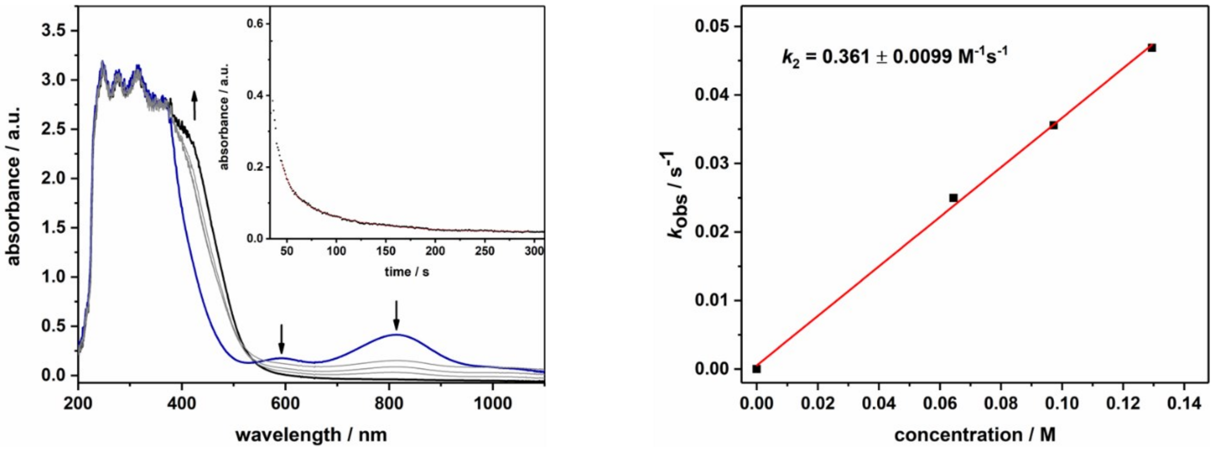

Figure S8. Left: Changes in the UV-Vis absorption spectra of a 1 mM solution of **1-*trans*** (blue line) in CH_2Cl_2/CH_3CN at -80 °C upon addition of 97 eq cyclohexa-1,4-diene (1,4-CHD); inset shows time trace for the decay of the 815 nm band and its pseudo-first order fit. Right: Plots of the pseudo-first order rate constants k_{obs} vs the substrate concentrations for 1,4-CHD in order to determine the second-order rate constant k_2 for the reaction of **1-*trans*** with 1,4-CHD.

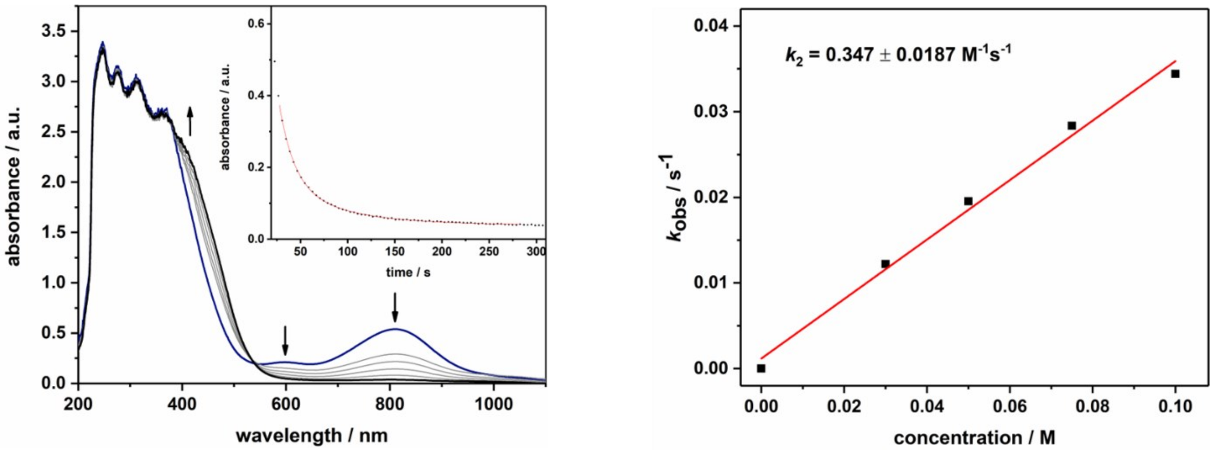

Figure S9. Left: Changes in the UV-Vis absorption spectra of a 1 mM solution of **1-*trans*** (blue line) in CH_2Cl_2/CH_3CN at -80 °C upon addition of 100 eq 9,10-Dihydroanthracene (DHA); inset shows time trace for the decay of the 815 nm band and its pseudo-first order fit. Right: Plots of the pseudo-first order rate constants k_{obs} vs the substrate concentrations for DHA in order to determine the second-order rate constant k_2 for the reaction of **1-*trans*** with DHA.

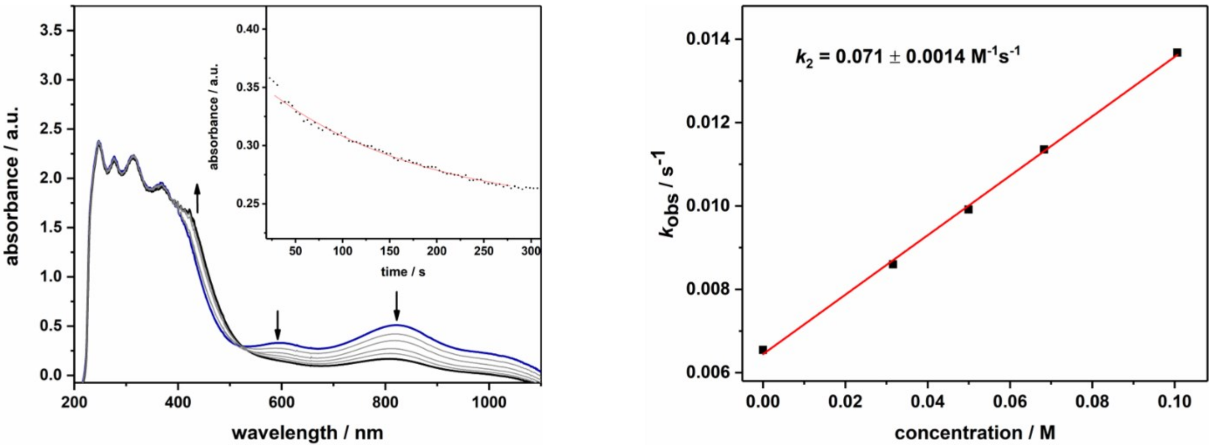

Figure S10. Left: Changes in the UV-Vis absorption spectra of a 1 mM solution of **1-*trans*** (blue line) in CH_2Cl_2/CH_3CN (95:5) at -65 °C upon addition of 68 eq fluorene; inset shows time trace for the decay of the 815 nm band and its pseudo-first order fit. Right: Plots of the pseudo-first order rate constants k_{obs} vs the substrate concentrations for fluorene in order to determine the second-order rate constant k_2 for the reaction of **1-*trans*** with fluorene.

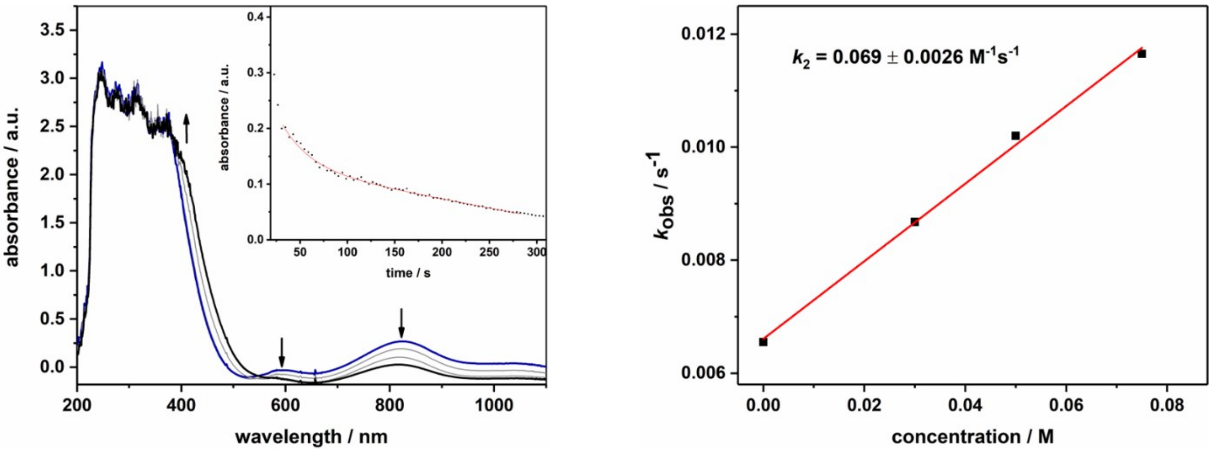

Figure S11. Left: Changes in the UV-Vis absorption spectra of a 1 mM solution of **1-*trans*** (blue line) in CH_2Cl_2/CH_3CN (95:5) at -65 °C upon addition of 75 eq indene; inset shows time trace for the decay of the 815 nm band and its pseudo-first order fit. Right: Plots of the pseudo-first order rate constants k_{obs} vs the substrate concentrations for indene in order to determine the second-order rate constant k_2 for the reaction of **1-*trans*** with indene.

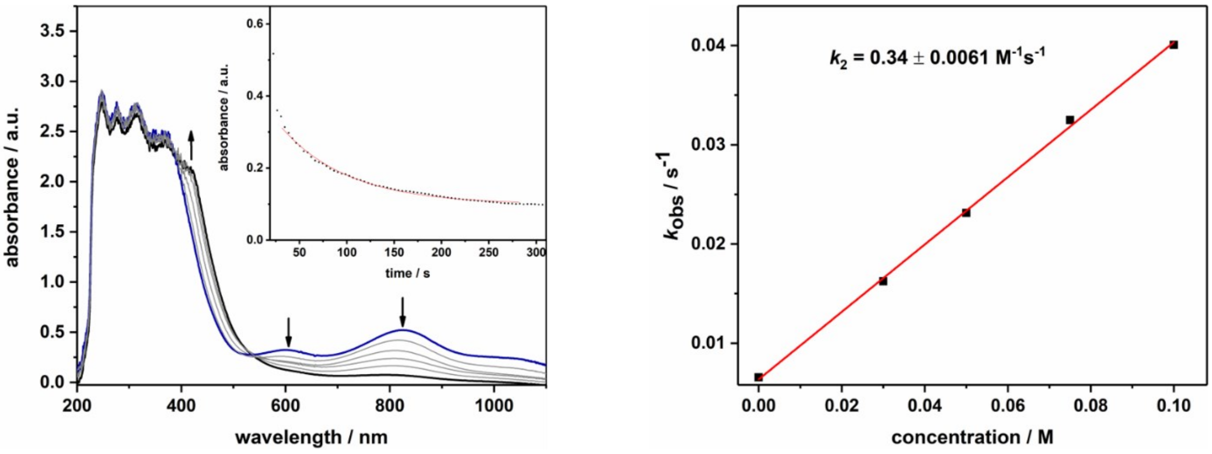

Figure S12. Left: Changes in the UV-Vis absorption spectra of a 1 mM solution of **1-*trans*** (blue line) in CH_2Cl_2/CH_3CN (95:5) at -65 °C upon addition of 30 eq thioanisole; inset shows time trace for the decay of the 815 nm band and its pseudo-first order fit. Right: Plots of the pseudo-first order rate constants k_{obs} vs the substrate concentrations for thioanisole in order to determine the second-order rate constant k_2 for the reaction of **1-*trans*** with thioanisole.

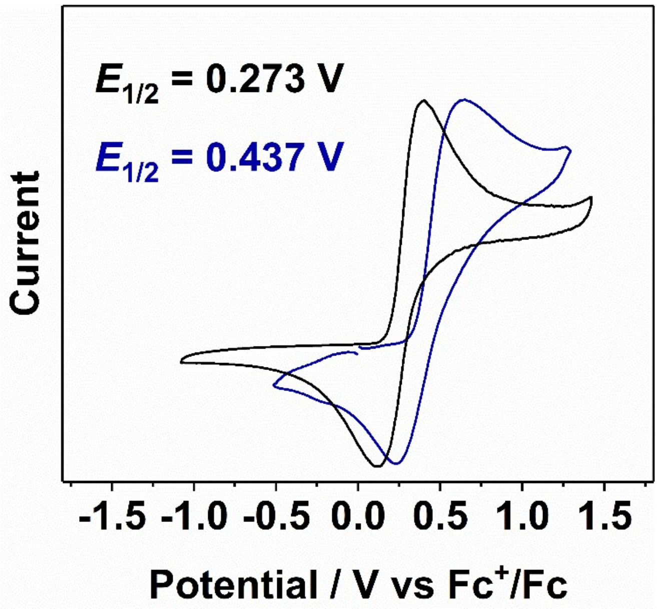

Figure S13. Cyclic voltammogramms of **1a-*trans*** (blue) and **2a-*trans*** (black) in anhydrous CH_3CN at 25 °C under inert conditions vs Fc^+/Fc.

Table S5. DFT/BP86/TZVP calculations on **1-*trans*** and **2-*trans*** in *S* = 1 and *S* = 2 states**.** The ground state is *S* = 1 as also obtained experimentally. The values highlighted in bold represents the lowest energy structures.

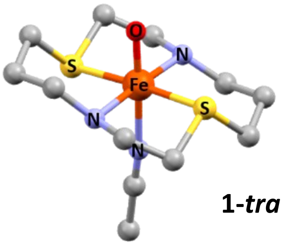

1-*trans*; S=1

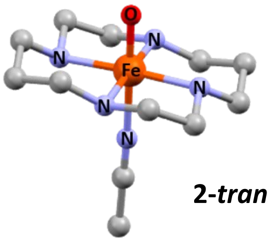

2-*trans*; S=1

model	S	Fe=O [Å]	Fe-N [Å]	Fe-N [Å]	Fe-N/S [Å]	Fe-N/S [Å]	Fe-NCMe [Å]	E [a.u.]	ΔE [kJ/mol]
1-*trans*	**1**	**1.657**	**2.057**	**2.060**	**2.292**	**2.305**	**2.029**	**-2772.3319**	**0.0**
1-*trans*	2	1.647	2.173	2.175	2.497	2.508	2.041	-2772.2992	85.9
2-*trans*	**1**	**1.655**	**2.031**	**2.033**	**2.033**	**2.031**	**2.037**	**-2086.6158**	**0.0**
2-*trans*	2	1.649	2.135	2.137	2.138	2.135	2.029	-2086.5742	109.1

Table S6. DFT/BP86/TZVP calculations on **1-*trans*** and **2-*trans*** with fixed Fe=O distances. **1-*trans***_opt and **2-*trans***_opt represents the structure with minimum energy as obtained by geometry optimizations in the *S* = 1 state. The values highlighted in red represent the ones that can best account for the experimental ν(Fe-O) values.

model	Energy [a.u.]	Relative Energies [kJ/mol]	Fe-O [Å]	ν(Fe-O) [cm^{-1}]
1-*trans*_opt	-2772.3319	0.00	1.657	852.1
1-*trans*_166	-2772.3319	0.02	1.660	843.1
1-*trans*_167	-2772.3318	0.27	1.670	820.5
1-*trans*_168	-2772.3316	0.82	1.680	793.7
1-*trans*_169	-2772.3312	1.64	1.690	771.6
1-*trans*_170	-2772.3308	2.73	1.700	749.0
2-*trans*_opt	-2086.6158	0.00	1.655	854.0
2-*trans*_166	-2086.6158	0.04	1.660	842.7
2-*trans*_167	-2086.6157	0.35	1.670	820.4
2-*trans*_168	-2086.6154	0.96	1.680	794.3
2-*trans*_169	-2086.6151	1.85	1.690	770.1
2-*trans*_170	-2086.6146	3.00	1.700	748.6

Table S7. Spectroscopic properties of **1-*trans*** and **2-*trans***.

	1-*trans*	**2-*trans***
Fe=O stretch	793 cm^{-1}	842 cm^{-1}
Fe-N (ligand) distances	1.88 Å	2.01 Å
Fe-S distances	2.25 Å	-
Fe-N (CH_3CN) distance	2.01 Å	2.10 Å
Fe-O distance (EXAFS)	1.67±0.01 Å	1.67±0.01 Å
Fe K-edge energy	7122.7 eV	7123.9 eV
MB parameters	ΔE_Q = 1.21 mms^{-1}, δ = 0.13 mms^{-1}	ΔE_Q = 2.49 mms^{-1}, δ = 0.05 mms^{-1}
UV-Vis features	596 nm, 815 nm	582 nm, 690 nm

References

1. Sheldrick, G. M. *SADABS*, University of Göttingen, Germany, 2002.
2. Sheldrick, G. M., SHELXT–Integrated space-group and crystal-structure determination. *Acta Crystallographica Section A: Foundations and Advances* **2015,** *71* (1), 3-8.
3. Sheldrick, G. M., Crystal structure refinement with SHELXL. *Acta Crystallographica Section C: Structural Chemistry* **2015,** *71* (1), 3-8.
4. Hübschle, C. B.; Sheldrick, G. M.; Dittrich, B., ShelXle: a Qt graphical user interface for SHELXL. *Journal of applied crystallography* **2011,** *44* (6), 1281-1284.
5. Spek, A. L., Structure validation in chemical crystallography. *Acta Crystallographica Section D: Biological Crystallography* **2009,** *65* (2), 148-155.
6. Kass, D.; Corona, T.; Warm, K.; Braun-Cula, B.; Kuhlmann, U.; Bill, E.; Mebs, S.; Swart, M.; Dau, H.; Haumann, M., Stoichiometric Formation of an Oxoiron (IV) Complex by a Soluble Methane Monooxygenase Type Activation of O2 at an Iron (II)-Cyclam Center. *Journal of the American Chemical Society* **2020,** *142* (13), 5924-5928.
7. Dau, H.; Liebisch, P.; Haumann, M., X-ray absorption spectroscopy to analyze nuclear geometry and electronic structure of biological metal centers—potential and questions examined with special focus on the tetra-nuclear manganese complex of oxygenic photosynthesis. *Analytical and bioanalytical chemistry* **2003,** *376* (5), 562-583.
8. Rehr, J. J.; Kas, J. J.; Vila, F. D.; Prange, M. P.; Jorissen, K., Parameter-free calculations of X-ray spectra with FEFF9. *Physical Chemistry Chemical Physics* **2010,** *12* (21), 5503-5513.
9. Walker, T. L.; Malasi, W.; Bhide, S.; Parker, T.; Zhang, D.; Freedman, A.; Modarelli, J. M.; Engle, J. T.; Ziegler, C. J.; Custer, P., Synthesis and characterization of 1, 8-dithia-4, 11-diazacyclotetradecane. *Tetrahedron Letters* **2012,** *53* (48), 6548-6551.
10. Macikenas, D.; Skrzypczak-Jankun, E.; Protasiewicz, J. D., A new class of iodonium ylides engineered as soluble primary oxo and nitrene sources. *Journal of the American Chemical Society* **1999,** *121* (30), 7164-7165.
11. Frisch, M.; Trucks, G.; Schlegel, H.; Scuseria, G.; Robb, M.; Cheeseman, J.; Scalmani, G.; Barone, V.; Petersson, G.; Nakatsuji, H., Gaussian 16, revision C. 01. Gaussian, Inc., Wallingford CT: 2016.
12. Grimme, S.; Antony, J.; Ehrlich, S.; Krieg, H., A consistent and accurate ab initio parametrization of density functional dispersion correction (DFT-D) for the 94 elements H-Pu. *The Journal of chemical physics* **2010,** *132* (15), 154104.